

## Shubnikov-de Haas Effect in Lithium-Diffused Tellurium-Doped *n*-Type Gallium Antimonide\*

T. O. YEP AND W. M. BECKER

*Department of Physics, Purdue University, Lafayette, Indiana*

(Received 29 November 1965)

Shubnikov-de Haas oscillations in magnetoresistance have been observed in low-concentration *n*-type tellurium-doped gallium antimonide after lithium diffusion. The Fermi energies of the samples investigated lie between  $\sim 0.03$  and  $\sim 0.05$  eV above the  $\mathbf{k}=0$  conduction-band minimum. Since the energy difference between the  $\mathbf{k}=0$  minimum and subsidiary  $\langle 111 \rangle$  minima is  $\sim 0.08$  eV at  $4.2^\circ\text{K}$ , the oscillatory effect is due solely to carriers in the  $\mathbf{k}=0$  valley. The oscillatory behavior has been investigated over the temperature range 1.3 to  $20.4^\circ\text{K}$  in magnetic fields up to 29 KG. The carrier concentration derived from the period of oscillation is in good agreement with Hall-coefficient results. Analysis of oscillatory amplitude as a function of temperature for the lithium-diffused samples yields a smaller effective mass than was observed earlier for as-grown tellurium-doped material with a Fermi energy  $\sim 0.08$  eV above the  $\mathbf{k}=0$  minimum. The result is shown to be consistent with the nonparabolicity predicted by a Kane conduction-band model for the  $\mathbf{k}=0$  band. Nonthermal broadening is primarily collision broadening.

### I. INTRODUCTION

IN 1964, Shubnikov-de Haas oscillations were reported for tellurium-doped *n*-GaSb single crystals with  $n \geq 10^{18} \text{ cm}^{-3}$ .<sup>1</sup> The observation of the effect at moderate magnetic field strengths is consistent with the observed carrier mobilities in such samples. Extensive experimental investigation has shown that the lowest conduction band of GaSb is centered at  $\mathbf{k}=0$ , but there are subsidiary minima lying along  $\langle 111 \rangle$  directions which are close by in energy.<sup>2</sup> The energy separation of the two band edges is  $\sim 0.08$  eV at  $4.2^\circ\text{K}$ ; the electron concentration in the central band corresponding to a Fermi level position of 0.08 eV is  $n \sim 10^{18} \text{ cm}^{-3}$ . Thus the magnetoresistance oscillations so far observed in *n*-GaSb occur for Fermi levels close to or inside the subsidiary minima. On the basis of effective-mass and carrier-concentration values obtained from the data, it was concluded that the oscillatory effects are due to conduction by carriers in the  $\mathbf{k}=0$  valley. Magnetoresistance oscillations could not be observed in samples with  $n < 10^{18} \text{ cm}^{-3}$  at ordinary fields because of the large increase in nonthermal damping for Fermi levels below 0.08 eV. The large decrease in damping as the Fermi level nears the second band indicates that the damping is not due to the central band alone, but is influenced by the presence of the second band as well. Several mechanisms involving two-band conduction were offered to explain the damping behavior for Fermi levels close to the subsidiary minima. These included (1) oscillatory transfer of carriers between the  $\langle 111 \rangle$  valleys and the central band, (2) screening of impurity ions by the heavy mass carriers in the side bands, and (3) suppression of inhomogeneity effects because of the large

density of states in the  $\langle 111 \rangle$  valleys. According to calculations, the first effect appears to be too small to account for the observed amplitudes. The relative importance of the second and third mechanisms could not be determined from the data.

In Te-doped *n*-GaSb, the carrier mobilities at  $4.2^\circ\text{K}$  drop sharply with decreasing carrier concentration for  $n \lesssim 0.9 \times 10^{18} \text{ cm}^{-3}$ . The cyclotron-resonance condition cannot be attained in such samples except at excessively high magnetic fields; favorable observation of the Shubnikov-de Haas effect in this case is extremely unlikely.

Yep and Becker reported recently that a considerable increase in  $4.2^\circ\text{K}$  carrier mobilities can be effected in samples with  $n \sim 1 - 4 \times 10^{17} \text{ cm}^{-3}$  by diffusing lithium into low-concentration as-grown Te-doped *n*-GaSb.<sup>3</sup> The cyclotron-resonance condition is then satisfied at ordinary magnetic field strengths in the lithium-diffused material. Since the increase in the momentum relaxation time is expected to be accompanied by a decrease in collision broadening, the observation of the Shubnikov-de Haas effect becomes favorable for Fermi-level positions well below the  $\langle 111 \rangle$  valley edges.

The present paper reports the results of an investigation of the Shubnikov-de Haas effect in low-concentration lithium-diffused Te-doped *n*-GaSb in the temperature range 1.3 to  $20.4^\circ\text{K}$ . Observation of the oscillations at low concentrations directly establishes that the effect is due to carriers in the central band. The data indicate possible nonparabolicity of the central conduction band; the result is shown to be consistent with an appropriate Kane conduction-band model. Inhomogeneity effects are found to be minor, and nonthermal broadening appears to be determined primarily by collision broadening.

### II. THEORY

With the application of a magnetic field the quasi-continuous distribution of energy levels in the conduc-

\* Work supported in part by the Advanced Research Projects Agency and the U. S. Army Research Office, Durham, North Carolina.

<sup>1</sup> W. M. Becker and H. Y. Fan, in *Proceedings of the International Conference on the Physics of Semiconductors, Paris, 1964* (Dunod Cie., Paris, 1964), p. 663.

<sup>2</sup> W. M. Becker, A. K. Ramdas, and H. Y. Fan, *J. Appl. Phys. Suppl.* **32**, 2094 (1961); A. Sagar, *Phys. Rev.* **117**, 93 (1960).

<sup>3</sup> T. O. Yep and W. M. Becker, *J. Appl. Phys.* **37**, 456 (1966).

tion band is split up into Landau-level sub-bands, the density of states becoming infinite at the bottom of each sub-band. The energy separation between the minima of successive Landau levels is equal to the cyclotron-resonance quantum of energy  $\hbar\omega_c$  and the  $n$ th Landau level lies a distance  $(n+\frac{1}{2})\hbar\omega_c$  above the zero-field band edge, where  $n$  has integer values. This effect arises from the quantization of the orbital motion of the electrons in the plane perpendicular to the magnetic field. Changes in the magnetic field result in the passage of the Landau levels past the Fermi energy. As a result, oscillations in magnetic susceptibility, and in transport properties, such as magnetoresistance, occur which are periodic in reciprocal magnetic field.

The conditions necessary for the oscillatory effects to be observed are the following:

$$\omega_c\tau \gg 1, \quad (1a)$$

$$\hbar\omega_c > k_B T, \quad (1b)$$

$$\zeta > \hbar\omega_c, \quad (1c)$$

where  $\omega_c = eB/m^*c$ ;  $m^*$  represents the cyclotron effective mass,  $B$  is the magnetic field strength,  $\tau$  is the relaxation time or quantum state lifetime,  $k_B$  is the Boltzmann constant, and  $\zeta$  is the zero-field Fermi energy. According to the first condition, for the Landau levels to be distinct, their energy separation  $\hbar\omega_c$  must be larger than the energy broadening of each level  $\hbar/\tau$  arising from the uncertainty principle. The condition (1a) may also be expressed in the form  $\mu B \gg 10^8$ , where  $\mu$  is the Hall mobility in  $\text{cm}^2/\text{volt sec}$  and  $B$  is the magnetic field in gauss. Relation (1b) expresses the requirement that the carriers be degenerate so that the conductivity depends sensitively on the density of states at the Fermi level. Condition (1c) places a limit on the maximum magnetic field beyond which no further oscillations would be expected.

The theory of the transverse magnetoconductivity oscillations for both acoustical lattice scattering and ionized impurity scattering has been developed by Adams and Holstein for spherical energy surfaces.<sup>4</sup> For both mechanisms they have found that the relative amplitudes of the oscillations for both ionized impurity scattering and acoustical lattice scattering are essentially the same. Using their expression for the oscillatory behavior of the conductivity, the oscillations in the transverse magnetoresistance can be expressed to a good approximation by

$$\frac{\Delta\rho_{xx}}{\rho_0} = (5\sqrt{2})\pi^2 \frac{k_B T}{(\hbar\omega_c\zeta)^{1/2}} \sum_{M=1}^{\infty} \frac{(-1)^M M^{1/2} e^{-2\pi^2 k_B T' M / \hbar\omega_c}}{\sinh(2\pi^2 k_B T M / \hbar\omega_c)} \times \cos\left(\frac{2\pi\zeta M}{\hbar\omega_c} - \frac{\pi}{4}\right) \quad (2)$$

<sup>4</sup> E. N. Adams and T. A. Holstein, *J. Phys. Chem. Solids* **10**, 254 (1959).

for cases where the deviation of the mean dc conductivity and magnetoresistance from their respective zero-field values is small. In Eq. (2),  $\rho_0$  is the zero-field resistivity,  $M$  denotes the  $M$ th harmonic of the oscillation, and  $T'$  is the nonthermal broadening temperature. The  $T'$  is related to the collision broadening relaxation time by the expression

$$T' = \hbar/\pi k_B \tau.$$

Recent experimental work indicates that inhomogeneities may produce exponential damping of the oscillations, so that  $T'$  values determined from experiment may reflect both collision broadening and inhomogeneity broadening.<sup>5</sup>

In treating the oscillatory longitudinal magnetoconductivity, Argyres<sup>6</sup> obtained an expression very similar to that of Adams and Holstein.<sup>4</sup> From Argyres' equation the longitudinal magnetoresistance oscillations, for situations where the changes in resistivity from the zero-field value are small, are accurately given by

$$\frac{\Delta\rho_{zz}}{\rho_0} = \pi^2 \sqrt{2} \frac{k_B T}{(\hbar\omega_c\zeta)^{1/2}} \sum_{M=1}^{\infty} \frac{(-1)^M M^{1/2} e^{-2\pi^2 k_B T' M / \hbar\omega_c}}{\sinh(2\pi^2 k_B T M / \hbar\omega_c)} \times \cos\left(\frac{2\pi\zeta M}{\hbar\omega_c} - \frac{\pi}{4}\right). \quad (3)$$

The exponential nonthermal broadening term is added to Argyres' equation to account for collision and inhomogeneity broadening. For the band parameters of GaSb the higher harmonic terms in Eqs. (2) and (3) can be shown to be negligible for the magnetic fields used in the current investigation, and only the term for  $M=1$  need be considered.

The period of the oscillations is inversely proportional to the extremal cross section  $S$  of the Fermi surface perpendicular to the magnetic field and is given by<sup>7</sup>

$$\Delta(1/B) = (2\pi e/\hbar c S) \text{ gauss}^{-1}. \quad (4)$$

On the assumption that the central conduction band is spherical, the period may be expressed in terms of the carrier concentration  $N$  as

$$\Delta(1/B) = (2e/\hbar c) (3\pi^2 N)^{-2/3} = (3.18 \times 10^6 / N^{2/3}) \text{ gauss}^{-1}. \quad (5)$$

### III. EXPERIMENT

The Te-doped  $n$ -type GaSb single crystals used in this study were grown by the Czochralski technique. Unoriented samples were taken from slices cut perpendicular to the ingot growth axis. In the case of samples No. 3, No. 11, and No. 13, the ingot was grown in the

<sup>5</sup> K. F. Cuff, M. R. Ellett, and C. D. Kuglin, *J. Appl. Phys. Suppl.* **32**, 2179 (1961).

<sup>6</sup> P. N. Argyres, *J. Phys. Chem. Solids* **4**, 19 (1958).

<sup>7</sup> J. M. Ziman, *Electrons and Phonons* (Oxford University Press, New York, 1960), p. 523.

TABLE I. Hall coefficient  $R_H$  in  $\text{cm}^2 \text{coulomb}^{-1}$  and Hall mobility  $\mu_H$  in  $\text{cm}^2 \text{volt}^{-1} \text{sec}^{-1}$  at  $4.2^\circ\text{K}$  before and after lithium diffusion.

Sample	$R_H$		$\mu_H$	
	Before	After	Before	After
No. 3	-17.4	-14.1	$4.80 \times 10^8$	$6.65 \times 10^8$
RA-2		-16.9		$7.13 \times 10^8$
No. 11	-34.0	-22.7	$3.14 \times 10^8$	$6.46 \times 10^8$
No. 13	-50.5	-30.1	$3.07 \times 10^8$	$5.23 \times 10^8$

$\langle 110 \rangle$  direction. The samples were approximately  $15 \times 1.5 \times 1$  mm in size after being lapped and etched. Two current and four potential leads were applied to the sample using cerroseal solder. Hall-coefficient measurements using two pairs of contacts and point-by-point resistivity probe measurements were carried out before and after lithium diffusion in order to determine sample homogeneity. For the case of the three samples mentioned above, Hall-coefficient values agreed to within 10% for pairs of probes separated by approximately 6 mm; the same degree of homogeneity was also indicated from the resistivity probe results. R. D. Baxter of the Battelle Memorial Institute kindly made available to us an unoriented sample of lithium-diffused material, designated as RA-2, which we have included in the present investigation. Hall-effect and resistivity measurements on this sample also indicated homogeneity to within approximately 10% after lithium diffusion.

Voltage measurements have been carried out using conventional dc potentiometric techniques. Magnetic field strengths up to 29 kG were obtained using a Pacific Electric Motor electromagnet. A Rawson Model No. 720 rotating coil fluxmeter was used to measure the magnetic field. The fluxmeter was periodically calibrated against a Rawson standard magnet having a field strength of 2.660 kG. Samples were immersed directly in the refrigerants during the low-temperature measurements. Temperatures from 20.4 to  $9.3^\circ\text{K}$  were obtained by pumping on liquid hydrogen and from 4.2 to  $1.3^\circ\text{K}$  by pumping on liquid helium.

Table I lists the Hall-coefficient and carrier mobility

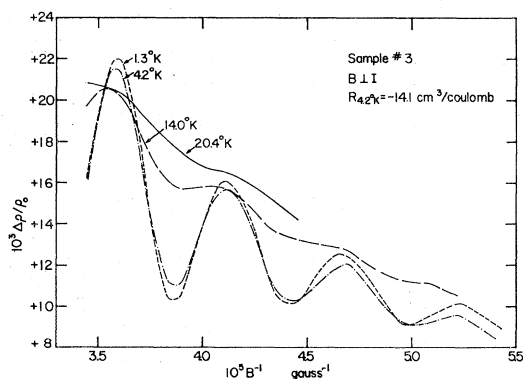


FIG. 1. Transverse magnetoresistance oscillations for sample No. 3.

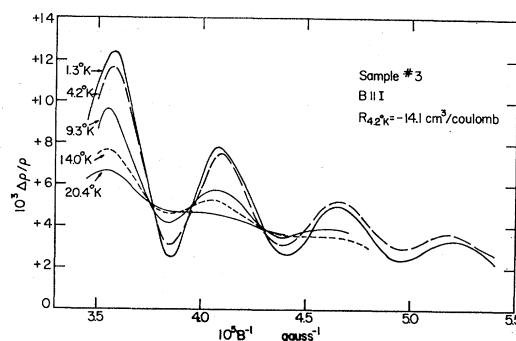


FIG. 2. Longitudinal magnetoresistance oscillations for sample No. 3.

values of the samples before and after lithium diffusion. The technique of lithium diffusion employed has been described previously.<sup>3</sup> Samples No. 3, No. 11, and No. 13 were lithium diffused for one week at  $500^\circ\text{K}$ , whereas sample RA-2 was lithium diffused for only three days at  $400^\circ\text{K}$ . As seen from Table I, both the mobility and carrier concentration increase as a result of lithium diffusion. The explanation for the result has been given in terms of an ion-pairing mechanism between lithium donor interstitials and compensating acceptor centers present in the as-grown Te-doped material.<sup>3</sup> Only 65% of the field strength is required to satisfy the cyclotron-resonance condition in the samples listed as compared to the values necessary for undiffused samples having the same Fermi energies as the diffused samples.

#### IV. RESULTS AND ANALYSIS

Figures 1 and 2 show the Shubnikov-de Haas effect for sample No. 3 with the current directions respectively transverse and longitudinal to the magnetic field direction for various temperatures between 1.3 and  $20.4^\circ\text{K}$ . Similar oscillatory behavior has also been observed in samples RA-2, No. 11, and No. 13. The oscillatory effect in the lowest concentration sample used in this investigation, sample No. 13, is shown in Fig. 3. Comparison of the first two figures with Fig. 3 clearly

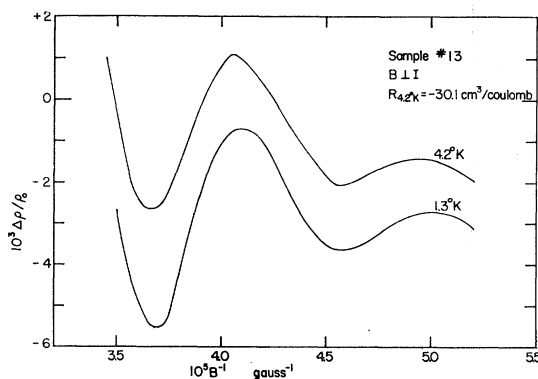


FIG. 3. Transverse magnetoresistance oscillations for sample No. 13.

illustrates that the period increases with decreasing carrier concentration. The smooth curves presented in the figures have been drawn through data points obtained by point-by-point potentiometric measurements; the actual data points have been deleted for the sake of clarity. For both the longitudinal and transverse orientations, the oscillations appear to be periodic in reciprocal field. We ignore the nonoscillatory component of both the longitudinal and transverse effects in our subsequent analysis, since it is not germane to the purposes of this paper.

### A. Amplitude

As will be brought out in our results, the nonthermal broadening is very nearly the same for both the longitudinal and transverse oscillatory amplitudes in each sample. Thus, intercomparison of the amplitudes at both orientations is valid at any field strength. Inspection of the figures shows that the ratio of the transverse to longitudinal amplitudes is greater than one, but never exceeds two, in contradiction to the theoretically predicted value of five from Eqs. (2) and (3). The experimental values of the amplitudes agree to within a factor of 3 with the theoretical prediction. However, the measured transverse amplitudes are smaller than the values predicted by Eq. (2), whereas the measured longitudinal amplitudes are larger than the values predicted by Eq. (3).

### B. Period

In the determination of the period of the oscillations, the reference level of the amplitude is taken to be the midpoint curve of the envelope of the oscillations; the nodal points correspond to the intersections of the oscillations with the midpoint curve. In Fig. 4 are

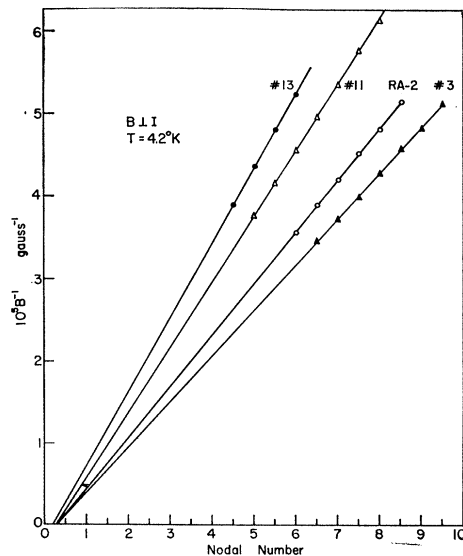


FIG. 4. Nodal points versus integers.

plotted the 4.2°K positions of the nodal points given in reciprocal field strength versus half integers. The slope of such plots is equal to the average period of the oscillations. The observed longitudinal and transverse oscillatory periods obtained at several different temperatures are tabulated in Table II.

For each sample, the periods measured at different temperatures and different current-magnetic field orientations are in very close agreement with each other. At low temperatures and for the carrier concentrations in the samples under investigation, the carriers remain in the  $k=0$  band and are degenerate. We have, therefore, determined the carrier concentration from  $N=1/|R_{4.2^\circ\text{K}}|e$ . The period of oscillations calculated from the Hall effect is seen to be in good agreement with the measured periods.

### C. Effective Mass

#### 1. Experimental

The effective mass of the electrons in the central conduction band can be determined by an analysis of the temperature dependence of the amplitude of oscillation at a particular magnetic field. From Eq. (2) at  $T=0^\circ\text{K}$ ,

$$\frac{\Delta\rho_{xx}}{\rho_0} = -5 \left( \frac{\hbar\omega_c}{2\xi} \right)^{1/2} \exp[-2\pi^2 k_B T' / \hbar\omega_c] \times \cos\left( \frac{2\pi\xi}{\hbar\omega_c} \frac{\pi}{4} \right). \quad (6)$$

Normalizing the expression for the amplitude of oscillations  $A$  in Eq. (2) or (3) at a given temperature and magnetic field with respect to that at  $T=0^\circ\text{K}$  and assuming that  $T'$  is temperature-independent, one gets

$$A_{T \neq 0^\circ\text{K}} / A_{T=0^\circ\text{K}} = \chi / \sinh\chi, \quad (7)$$

TABLE II. Period of oscillations at various temperatures.

Sample	Temperature °K	Theoretical period gauss <sup>-1</sup>	Observed period	
			$B \perp I$ gauss <sup>-1</sup>	$B \parallel I$ gauss <sup>-1</sup>
No. 3	1.3	$5.56 \times 10^{-6}$	$5.38 \times 10^{-6}$	$5.43 \times 10^{-6}$
	4.2		$5.52 \times 10^{-6}$	$5.39 \times 10^{-6}$
	9.3			$5.33 \times 10^{-6}$
	14.0		$5.28 \times 10^{-6}$	$5.43 \times 10^{-6}$
	20.4			$5.33 \times 10^{-6}$
RA-2	1.3	$6.19 \times 10^{-6}$	$6.41 \times 10^{-6}$	
	4.2		$6.24 \times 10^{-6}$	
No. 11	1.3	$7.53 \times 10^{-6}$	$7.84 \times 10^{-6}$	$7.82 \times 10^{-6}$
	4.2		$7.93 \times 10^{-6}$	$7.72 \times 10^{-6}$
	9.3			$8.22 \times 10^{-6}$
	14.0		$7.95 \times 10^{-6}$	$7.98 \times 10^{-6}$
	20.4		$7.74 \times 10^{-6}$	
No. 13	1.3	$9.07 \times 10^{-6}$	$9.23 \times 10^{-6}$	
	4.2		$9.05 \times 10^{-6}$	

where

$$\chi = 2\pi^2 k_B T / \hbar \omega_c = 1.468 \times 10^5 (m^*/m_0) (T/B). \quad (8)$$

In order to compare the measured amplitude ratios with theory, it is necessary to obtain the 0°K amplitude from the data. This is accomplished by extrapolating the amplitude values at the measurement temperatures to 0°K, as was done for sample No. 3 in Fig. 5. The plot of  $\chi/\sinh\chi$  versus  $\chi$  is a universal theoretical curve for the parameters  $m^*/m_0$ ,  $T$ , and  $B$  contained in  $\chi$ . These parameters must be adjusted to fit the normalized experimental amplitudes to the theoretical curve. Since the experimental amplitudes at a particular  $B$  are already given for the various  $T$ , the proper fitting must be accomplished by the adjustment of the effective mass  $m^*$ . Such a procedure was used for samples No. 3, RA-2, and No. 11, but could not be carried out for No. 13 due to the lack of experimental results above 4.2°K. An illustration of this method is shown in Fig. 6 for a longitudinal orientation of sample No. 3. The value of  $m^* = 0.050m_0$  places the experimental points well to the right of the curve, while  $m^* = 0.043m_0$  appears to give a good fit to the curve. In Table III are listed the effective masses obtained for No. 3, RA-2, and No. 11 by the curve-fitting technique.

The relative error in the normalized amplitudes due to the uncertainties in the extrapolation to 0°K is the same at all temperatures, but the absolute error decreases for the smaller amplitude values at the higher temperatures. Also, at higher temperatures, the superposition of the experimental points on the theoretical curve is more sensitive to the choice of  $m^*$  than at 1.3 and 4.2°K. Thus, we consider the fit at the higher temperatures to be the more reliable criterion for determining the effective mass as compared to the low-temperature points.

The effective mass for No. 13 can be found by an alternative method. The ratio of the amplitudes of oscillation at two different temperatures can be expressed as

$$A_1/A_2 = (\chi_1/\sinh\chi_1)/(\chi_2/\sinh\chi_2), \quad (9)$$

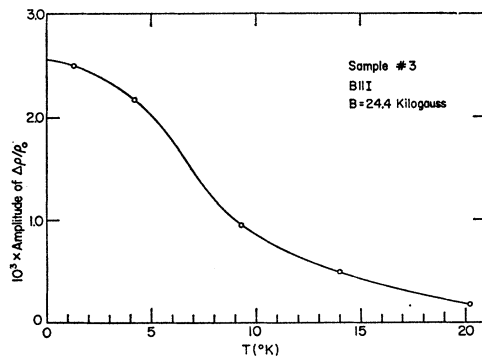


FIG. 5. Amplitude of oscillations versus temperature for sample No. 3.

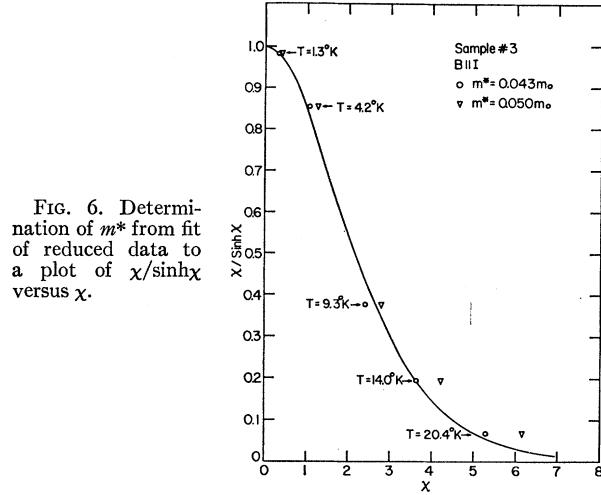


FIG. 6. Determination of  $m^*$  from fit of reduced data to a plot of  $\chi/\sinh\chi$  versus  $\chi$ .

where  $\chi_i = 2\pi^2 k_B T_i / \hbar \omega_c$ , the subscript  $i$  denoting the respective temperature. The transcendental Eq. (9) can be solved for  $m^*$  after substituting for the  $A$ 's the amplitudes of oscillation at 1.3 and 4.2°K at a particular magnetic field. For sample No. 13, we find  $m^* = 0.042 \pm 0.006m_0$  using amplitude values at 24.4 kG.

In obtaining Eqs. (8) and (9) the exponential term containing  $T'$  was eliminated by assuming that the collision broadening temperature  $T'$  is constant over the range of temperatures at which the oscillations are observed. But indeed, if  $T'$  is temperature-dependent between 0 and 20.4°K, then  $m^*$  would deviate from those values given in Table III. If  $T'$  increased with increasing temperature, the apparent  $m^*$  should decrease; while if  $T'$  decreases with increasing temperature, the apparent  $m^*$  should increase. For example, in the case of sample No. 3, an increase in  $T'$  of 0.5°K over the temperature range of 0 to 14°K would result in a change of  $m^*$  from  $0.043m_0$  to approximately  $0.041m_0$ . A decrease in  $T'$  of 0.5°K would increase the  $m^*$  value to approximately  $0.045m_0$ .

TABLE III. Comparison of experimentally measured effective masses with theoretically predicted mass values.

Sample	B kG	Measured $m^*$		Theoretical $m^*$ $\times 10^{-2}m_0$	Fermi energy $\times 10^{-2}$ eV
		$B \perp I$ $\times 10^{-2}m_0$	$B \parallel I$ $\times 10^{-2}m_0$		
No. 13	24.4	$4.2 \pm 0.6$		4.23 <sup>a</sup>	3.1
No. 11	24.4	$3.9 \pm 0.4$	$4.1 \pm 0.6$	4.31 <sup>a</sup>	3.5
RA-2	25.6	$3.9 \pm 0.5$		4.39 <sup>a</sup>	4.4
No. 3	24.4	$4.4 \pm 0.6$	$4.3 \pm 0.3$	4.46 <sup>a</sup>	5.0
Becker <i>et al.</i> <sup>d</sup>	25.0	$5.2 \pm 0.2$		4.91 <sup>a</sup>	8
Piller <sup>e</sup>		$4.9 \pm 0.5$	-0.3 <sup>b</sup>	4.4 <sup>b</sup>	4.6
Zwerdling <i>et al.</i> <sup>f</sup>	38.9	$4.7 \pm 0.3$ <sup>c</sup>		4.68 <sup>c</sup>	6.7

<sup>a</sup> Theoretical values obtained from Eq. (16) using method described in Sec. IV C. 2.  
<sup>b</sup> Electron susceptibility effective mass  $m_s^*$  measured by Faraday rotation. Theoretical value calculated by substituting Eq. (11) into definition of  $m_s^*$ , viz.,  $1/m_s^* = (1/\hbar^2) (1/k) (d\epsilon/dk)$ .  
<sup>c</sup> Cyclotron resonance electron effective mass obtained from oscillatory magnetoabsorption data. Theoretical value calculated from Eq. (16).  
<sup>d</sup> Reference 2.  
<sup>e</sup> Reference 14.  
<sup>f</sup> Reference 12.

## 2. Theoretical

The nonparabolicity of the conduction band in InSb was treated by Kane, who considered the interaction between the conduction band and valence bands for the  $\mathbf{k} \cdot \mathbf{p}$  perturbation and the  $\mathbf{k}$ -independent spin-orbit splitting.<sup>8</sup> Utilizing his secular equation, the conduction band of GaSb for the condition that  $E_c \ll (\frac{2}{3}\Delta + E_g)$  can be expressed as<sup>9</sup>

$$E = \frac{E_g}{2} + \frac{\hbar^2 k^2}{2m_0} + \left( \frac{E_g^2}{4} + \gamma^2 k^2 \right)^{1/2}, \quad (10a)$$

where  $E$  is the carrier energy relative to the valence-band edge,  $E_c$  is the carrier energy relative to the conduction-band minimum,  $\Delta$  is the spin-orbit splitting of the valence band,  $E_g$  is the energy gap,  $P$  is the momentum matrix element,  $m_0$  is the free-electron mass, and

$$\gamma^2 = P^2 (\frac{2}{3}\Delta + E_g) / (\Delta + E_g). \quad (10b)$$

The values of  $\Delta$  and  $E_g$ , as given by Ehrenreich,<sup>10</sup> are 0.86 and 0.813 eV, respectively, and the Fermi energy  $\zeta$  is less than 0.08 eV for all of the samples being considered. Thus, Eq. (10a) is applicable to our treatment. On rewriting Eq. (10a) and expanding for small energies, the carrier energy in the conduction band  $E_c$  is given by

$$E_c \sim \frac{\hbar^2 k^2}{2} \left( \frac{1}{m_0} + \frac{2}{\hbar^2 E_g} \gamma^2 \right) - \alpha \hbar^4 k^4 + \frac{2\gamma^6 \hbar^6}{E_g^2}, \quad (11)$$

where

$$\alpha = \gamma^4 / \hbar^4 E_g^3. \quad (12)$$

The band-edge effective mass  $m_0^*$  may be defined as

$$m_0^* = m_0 / \left( 1 + \frac{2m_0}{\hbar^2 E_g} \gamma^2 \right). \quad (13)$$

Taking into account the nonparabolicity of the energy band, the Landau energy levels are given by<sup>11</sup>

$$E_c = (n + \frac{1}{2}) \frac{\hbar e B}{m_0^* c} + \frac{\hbar^2 k_z^2}{2m_0^*} - 4\alpha m_0^{*2} \left[ (n + \frac{1}{2}) \frac{\hbar e B}{m_0^* c} + \frac{\hbar^2 k_z^2}{2m_0^*} \right]^2, \quad (14)$$

where the  $n$  is the  $n$ th Landau level previously defined, and  $k_z$  is the carrier wave vector in the magnetic field direction. The energy difference between the minima of the  $(n+1)$ th and  $n$ th Landau level is

$$\frac{\hbar e B}{m^* c} = \frac{\hbar e B}{m_0^* c} \left[ 1 - 8\alpha m_0^{*2} \frac{\hbar e B}{m_0^* c} (n+1) \right]. \quad (15)$$

<sup>8</sup> E. O. Kane, J. Phys. Chem. Solids **1**, 249 (1957).

<sup>9</sup> M. Cardona, Phys. Rev. **121**, 752 (1961).

<sup>10</sup> H. Ehrenreich, J. Appl. Phys. Suppl. **32**, 2155 (1961).

<sup>11</sup> B. Lax and J. G. Mavroides, in *Solid State Physics*, edited by F. Seitz and D. Turnbull (Academic Press Inc., New York, 1960), Vol. 11, p. 361.

Here  $m^*$  may be considered to be an average effective mass over the energy range between the  $(n+1)$ th and  $n$ th Landau-level minima and  $\alpha$  is given by Eq. (12). The effective mass as measured by the Shubnikov-de Haas effect is then

$$m^* = m_0^* / [1 - 8\alpha m_0^{*2} (\hbar e B / m_0^* c) (n+1)]. \quad (16)$$

In order to make comparisons between experiment and the theoretical relation (16) above, it is necessary to determine the Landau level  $n'$  appropriate to the magnetic field value at which the effective mass was obtained experimentally. The correct value of the particular Landau level  $n'$  associated with a magnetic field  $B$  is found by the following procedure: The minimum of the  $n'$ th Landau level is considered to be at the Fermi energy  $\zeta$ . From Eq. (4), the wave vector at the Fermi energy  $k_F$  can be obtained from the period of oscillation  $\Delta(1/B)$  by

$$k_F^2 = 2e / [\hbar c \Delta(1/B)]. \quad (17)$$

If  $\gamma^2$  is known, the Fermi energy can be calculated by evaluating Eq. (11) for  $k$  equal to  $k_F$ . If  $m_0^*$  is determined,  $n'$  can be specified by adding the energy difference between the band minimum and the  $n=0$  level and the energy differences between successive levels, as given by Eq. (15), until their sum equals the Fermi energy, the final Landau level in the sum being the required  $n'$ . The effective mass at the Fermi energy is then the average of the  $m^*$ 's calculated for  $n+1=n'$  and  $n'+1$  in Eq. (16).

In order to calculate  $\zeta$ ,  $m_0^*$ , and  $m^*$ , a value for  $\gamma^2$  was obtained by utilizing the oscillatory magnetoabsorption data of Zwerdling, Lax, Button, and Roth.<sup>12</sup> From their line spectrum of the transmission oscillatory minima they obtained a cyclotron-resonance electron effective mass of  $0.047 \pm 0.003 m_0$ . Their experiment measures the electron effective mass in the vicinity of a Landau-level conduction-band minimum, which is at an energy  $\epsilon_c(n, B)$  above the zero-field conduction-band edge. To determine  $\gamma^2$  we must know the value of  $\epsilon_c$  for their measured value of the electron effective mass. The photon energy  $h\nu$  at a transmission minimum is related to  $\epsilon_c(n, B)$  by

$$\epsilon_c(n, B) = h\nu + E_x - E_g - \epsilon_v(n, B), \quad (18)$$

where  $E_x$  is the exciton binding energy,  $E_g$  is the energy gap, and  $\epsilon_v(n, B)$  is the energy maximum of the  $n$ th Landau level in the valence band. In obtaining their value of  $m^* = 0.047 m_0$ , Zwerdling *et al.* used the average energy difference for their fifth, sixth, seventh, and eighth lines in the  $\mathbf{E} \parallel \mathbf{B}$  spectrum. Thus, the average photon energy of the four lines is to be used for  $h\nu$  in Eq. (18). Although the exciton binding energy is in general magnetic-field-dependent, we take the binding energy for excitons in GaSb to be approximately

<sup>12</sup> S. Zwerdling, B. Lax, K. Button, and L. M. Roth, J. Phys. Chem. Solids **9**, 320 (1959).

0.0028 eV.<sup>13</sup> A value of  $E_g=0.813$  eV was obtained by Zwerdling *et al.* from their data. The remaining unknown quantity in Eq. (18) is  $\epsilon_c(n,B)$ . The specific quantum numbers  $n$  of the valence-band Landau levels associated with the fifth, sixth, seventh, and eighth lines in the absorption spectrum were not designated by the authors. We assume that these lines correspond to  $\Delta n=0$  transitions between the heavy-hole Landau level and the Landau levels in the  $\mathbf{k}=0$  conduction band. The average value of  $n$  for the four lines is 5.5 under the assumption that the fifth line corresponds to the  $n=4$  heavy-hole Landau level. On the other hand, the average  $n$  might be as low as 1.5 if the fifth line corresponds to the  $n=0$  heavy-hole Landau level. From Eq. (18), the average conduction-band energy of the final states for these transitions should be somewhere between  $\epsilon_c=0.0641$  eV and  $\epsilon_c=0.0689$  eV. Approximating  $n+1$  with  $\epsilon_c(\hbar eB/m_0^*c)^{-1}$  in Eq. (16) and also substituting Eqs. (13) and (12) into Eq. (16),  $m^*$  is expressed by

$$m^* = m_0 \left( 1 + \frac{2m_0\gamma^2}{\hbar^2 E_g} \right)^{-1} \times \left[ 1 - \frac{8\gamma^4 m_0^2 \epsilon_c}{\hbar^4 E_g^3} \left( 1 + \frac{2m_0\gamma^2}{\hbar^2 E_g} \right)^{-2} \right]^{-1}. \quad (19)$$

In Eq. (19), pairs of values of  $\gamma^2$  and  $\epsilon_c$  of  $7.39 \times 10^{-15}$  eV<sup>2</sup> cm<sup>2</sup> and 0.0641 eV, and  $7.49 \times 10^{-15}$  eV<sup>2</sup> cm<sup>2</sup> and 0.0689 eV, respectively, yield an  $m^*$  of  $0.047m_0$ . From Eq. (13),  $\gamma^2$  values of  $7.39 \times 10^{-15}$  eV<sup>2</sup> cm<sup>2</sup> and  $7.49 \times 10^{-15}$  eV<sup>2</sup> cm<sup>2</sup> yield conduction-band minimum effective masses of  $0.0402m_0$  and  $0.0397m_0$ , respectively. The error in the determination of  $m_0^*$  and  $\gamma^2$  due to the uncertainty in the assignment of the quantum numbers is slight, since the 7% difference in  $\epsilon_c$  results in only a 1.3% difference in both  $\gamma^2$  and  $m_0^*$ . Using the average of the two  $\gamma^2$  values discussed above and Eq. (10b), we find  $P$  to be  $9.48 \times 10^{-8}$  eV cm. This result is in agreement with other III-V compound values of  $P$ , which range from  $8-9.5 \times 10^{-8}$  eV cm.<sup>10</sup>

For each value of  $\gamma^2$  and for each sample, the Fermi level was calculated using Eq. (11) and the Shubnikov-de Haas mass  $m^*$  was calculated from Eq. (16). The values of  $\zeta$  and  $m^*$  obtained for each of the  $\gamma^2$ 's differed by only 1%. The average of both sets of calculations for  $\zeta$  and  $m^*$  are listed in Table III. Although nonparabolicity is indicated from the calculations, it is only slight for the energy range under discussion. In the case of the lithium-diffused samples, a comparison of the theoretical and experimental effective masses shown in Table III indicates reasonable agreement within the error of the measurements. Using a Faraday rotation measurement, Piller derived an electron susceptibility effective-mass value of  $0.049 (+0.005, -0.003)m_0$  for a

Fermi level of  $\sim 0.046$  eV.<sup>14</sup> The value of  $0.047 \pm 0.003m_0$  was obtained by Zwerdling *et al.* at an estimated conduction-band energy of 0.067 eV. Becker and Fan found an effective mass of  $0.052 \pm 0.002m_0$  at a Fermi energy of  $\sim 0.08$  eV from Shubnikov-de Haas data.<sup>1</sup> These various masses are also listed in Table III together with estimated values of carrier energy and the appropriate effective masses derived from the theory. Considering the experimental errors, all of the results obtained to date are seen to be consistent with the degree of nonparabolicity predicted by the theory.

#### D. Nonthermal Broadening

From Eqs. (2) and (3), the amplitude of the oscillations  $A$  is directly proportional to

$$\exp[-2\pi^2 k_B T' / \hbar \omega_c] [B^{1/2} \zeta^{1/2} \sinh(2\pi^2 k_B T / \hbar \omega_c)]^{-1}.$$

Thus, a plot of  $\log_{10}[AB^{1/2}\zeta^{1/2} \sinh(2\pi^2 k_B T / \hbar \omega_c)]$  versus  $1/B$  at a particular temperature should be a straight line with a slope proportional to the nonthermal broadening temperature  $T'$ . Figure 7 contains such plots for samples No. 3, RA-2, No. 11, and No. 13 at 4.2°K. Using an average effective mass of  $0.041m_0$  for all four samples, the values of  $T'$  determined at the various temperatures are shown in Table IV. In some cases, the determination of  $T'$  at the higher temperatures was not feasible because of increased thermal damping.

A momentum-relaxation-broadening temperature  $T_\mu'$  can be defined in terms of the Hall mobility  $\mu$  by the relation

$$T_\mu' = \hbar e / (\pi k_B m^* \mu). \quad (20)$$

$T_\mu'$  values calculated for an average effective mass of  $m^*=0.041m_0$  are listed in Table IV. In each sample  $\mu$ ,

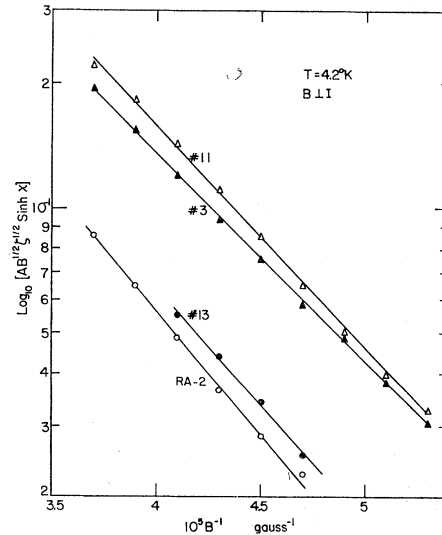



Fig. 7. Determination of nonthermal broadening temperature  $T'$  from a plot of  $\log_{10}[AB^{1/2}\zeta^{1/2} \sinh x]$  versus  $B^{-1}$ .

<sup>13</sup> E. J. Johnson, Ph.D. thesis, Purdue University, 1964 (unpublished).

<sup>14</sup> H. Piller, J. Phys. Chem. Solids 24, 425 (1963).


 TABLE IV. Nonthermal broadening temperatures  $T'$  related to momentum relaxation  $T_{\mu}'$ , and their ratios.

		No. 3				RA-2				No. 11				No. 13	
$T$ (°K)		1.3	4.2	14.0	20.4	1.3	4.2	14.0	17.0	1.3	4.2	14.0	20.4	1.3	4.2
$T'$ (°K)	$B \perp I$	19.0	19.4			23.8	23.3	11.8	21.2	19.9	20.3	21.8	19.7	25.7	21.8
	$B \parallel I$	19.6	18.7	20.4						18.7	20.3	22.6	34.9		
$T_{\mu}'$ (°K)		15.7	15.7	15.5	15.5	14.8	14.6	14.5	14.5	16.1	16.1	16.7	15.7	19.9	19.9
$\frac{T'}{T_{\mu}'}$	$B \perp I$	1.21	1.23			1.62	1.59	0.81	1.46	1.23	1.26	1.31	1.25	1.29	1.09
	$B \parallel I$	1.25	1.19	1.32						1.16	1.26	1.35	2.22		

and consequently  $T_{\mu}'$ , is essentially constant over the temperature range 1.3 to 20.4°K. The analysis of the oscillatory amplitude indicates that  $T'$  is essentially constant in the temperature range 1.3 to 4.2°K, whereas the results at the higher temperatures are not clear. Robinson and Rodriguez have calculated the temperature variation of  $T'$  and  $T_{\mu}'$  for various carrier concentrations using a model of ionized impurity scattering.<sup>15</sup> Their results show that for electron concentrations less than  $6.40 \times 10^{17} \text{ cm}^{-3}$ , both  $T'$  and  $T_{\mu}'$  vary by  $< 10^{-2} \text{°K}$  over the temperature range 0 to 30°K.<sup>16</sup> Thus, the experimentally observed temperature dependence of  $T_{\mu}'$  between 1.3 and 20.4°K and of  $T'$  between 1.3 and 4.2°K is in agreement with the theory. Also, the prediction that  $T'$  should be independent of temperature at and below 20.4°K justifies our assumption concerning  $T'$  in deriving Eq. (7) for the determination of the effective mass.

In Sec. IV. A, comparison of the ratio of the longitudinal to the transverse amplitude at fixed field was justified on the basis that the associated nonthermal damping was the same for both orientations. Inspection of the data in Table IV indicates that the comparison is valid for sample temperature  $T \leq 4.2 \text{°K}$ .

The  $T'/T_{\mu}'$  ratios calculated by Robinson and Rodriguez are of the order of three for the carrier concentrations found in our samples, whereas experimentally the ratios are between one and two, as seen in Table IV. The reasons for this discrepancy are not readily apparent from a consideration of the various features of the Robinson-Rodriguez model. Ratios of  $T'/T_{\mu}'$  of the order of one have been observed in other semiconductors.<sup>17,18</sup> Departures of the ratios to values greater than three have been assumed to indicate marked sample inhomogeneity.<sup>19</sup> By this criterion, then, the diffused samples used in this study appear to be

highly homogeneous. It may be noted that sample RA-2 exhibits a somewhat higher ratio of  $T'/T_{\mu}'$  at 1.3 and 4.2°K than the other samples listed. The result suggests that some inhomogeneity may be present in this sample because of incomplete dispersal of the lithium due to the shorter heating time and lower diffusion temperature as compared to the other samples discussed.

## V. SUMMARY

Shubnikov-de Haas oscillations in both the longitudinal and transverse magnetoresistance have been observed in  $n$ -GaSb single crystals for Fermi energy values well below the position corresponding to the  $\langle 111 \rangle$  valley edges. The samples exhibiting the oscillations were prepared by diffusing lithium into initially low-concentration tellurium-doped  $n$ -type material.

The oscillatory periods are found to be in good agreement with the values expected on the basis of Hall-coefficient data. The theoretical predictions of the amplitude of the oscillations are verified to within a factor of 3 by the experimental results.

The effective-mass values derived from the temperature dependence of the oscillations at a fixed magnetic field are somewhat smaller in low-concentration Li-diffused material than in high-concentration as-grown material. A Kane band calculation for the  $k=0$  conduction band, utilizing published magnetoabsorption data, suggests slight but significant nonparabolicity over the Fermi energy range 0.03–0.08 eV. The present experimental results, as well as other values of effective mass given in the literature, are found to be in reasonable agreement with the model.

Nonthermal broadening temperatures are close in value to damping temperatures expected on the basis of collision broadening. Inhomogeneity broadening appears to be negligible for the Li-diffusion techniques employed in the present study.

## ACKNOWLEDGMENTS

The authors gratefully acknowledge a valuable discussion with Professor H. Y. Fan, and the critical reading of this manuscript by Professor S. Rodriguez.

<sup>15</sup> J. E. Robinson and S. Rodriguez, Phys. Rev. **137**, A663 (1965).

<sup>16</sup> J. E. Robinson and S. Rodriguez (unpublished results).

<sup>17</sup> R. J. Sladek, Phys. Rev. **110**, 817 (1958).

<sup>18</sup> A. H. Kahn and H. P. R. Frederikse, in *Solid State Physics*, edited by F. Seitz and D. Turnbull (Academic Press Inc., New York, 1959), Vol. 9, p. 291.

<sup>19</sup> E. D. Hinkley and A. W. Ewald, Phys. Rev. **134**, A1261 (1964).